

Modeling and Numerical Simulation of a Brushless Permanent-Magnet DC Motor in Dynamic Conditions by Time-Stepping Technique

M. A. Jabbar, *Senior Member, IEEE*, Hla Nu Phyu, *Student Member, IEEE*, Zhejie Liu, *Senior Member, IEEE*, and Chao Bi, *Member, IEEE*

Abstract—A method of modeling and numerical simulation of a brushless permanent-magnet dc motor using time-stepping finite-element technique is presented. In the proposed model, the electromagnetic field equations, the stator circuit equation, and the motion equation are solved simultaneously at each time step; thus, the eddy-current effect, the saturation effect, the rotor movement, and the nonsinusoidal quantities can all be taken into account directly in the system of equations. Dynamic conditions of the motor at starting, step voltage variation, and load torque changes are investigated using the proposed dynamic model.

Index Terms—Brushless permanent-magnet dc (BLDC) motor, dynamic analysis, time-stepping finite-element method (FEM).

I. INTRODUCTION

THE dramatic improvement in power electronic switching devices, integrated circuits, developments and refinements in permanent-magnetic materials, and manufacturing technology have led to the development of brushless permanent-magnet motors that offer significant improvements in power density, efficiency, and noise reduction. Brushless permanent-magnet motors are especially demanded in clean and explosive environments such as aeronautics, robotics, food and chemical industries, electric vehicles, medical instruments, and computer peripherals. Hence, there has been an enormous interest in the analysis and design of brushless permanent-magnet motors in order to make them more efficient and more robust [1]–[7].

Prediction of motor performance is necessary for the evaluation of motor designs. Modeling and simulation is a preferred method in designing motors compared to building motor prototypes which is more costly [8]. With the advent of high-speed computing power and more powerful numerical methods in re-

cent years, it has become practical to use finite-element methods (FEMs) to compute the performance of electrical machines in both steady state as well as under transient and dynamic conditions [9]–[13]. Numerical simulation of electrical machines will be based on fewer assumptions to give a higher accuracy at the expense of computing requirements. The most powerful method for investigating the steady-state and dynamic performance is circuit-field-coupled time-stepping FEM which can couple the field equations with the motion and circuit equations and solve simultaneously at each time step. Therefore, the solution can take into account the saturation effect, the eddy-current effect, the rotor movement, and nonsinusoidal quantities that are very difficult to consider using analytical methods. Many empirical factors then become unnecessary [14], [17].

In this paper, modeling and numerical simulation of a brushless permanent-magnet dc (BLDC) motor using time-stepping FEM is presented. The proposed model has been successfully used to simulate the dynamic behavior of a BLDC motor at starting condition, changing of the mechanical load torque, and step voltage variations.

II. MODELING TECHNIQUE

In the time-stepping FEM model, the inputs are stator phase voltages, motor geometry, and material characteristics, whereas all the other variables such as magnetic vector potentials, currents, rotor positions, and the speed are calculated. The magnetic field equations for the stator and the rotor are written in their own coordinate systems. The solutions of the two field equations are matched with each other in the air gap. The rotor part of the FEM mesh is rotated at each time step by an angle determined from the motion equation.

A time-stepping FEM solver generally requires extensive computation time to overcome the starting period, especially when steady-state conditions have to be reached. In this paper, a *current-fed two-dimensional (2-D) complex eddy-current model* is developed first and the solutions gotten from this model are used as the initial conditions for the time-stepping FEM solver. Therefore, the computation time to overcome the starting period of steady-state conditions can be reduced.

A. Motor Topologies

A BLDC motor cannot work without electronic controllers. The terminal voltages on the stator windings of each phase are controlled by the power electronic switches. Two phases are

Paper IPCSD 04–010, presented at the 2003 IEEE International Electric Machines and Drives Conference, Madison, WI, June 1–4, and approved for publication in the IEEE TRANSACTIONS ON INDUSTRY APPLICATIONS by the Electric Machines Committee of the IEEE Industry Applications Society. Manuscript submitted for review July 29, 2003 and released for publication February 27, 2004.

M. A. Jabbar is with the Department of Electrical and Computer Engineering, National University of Singapore, Singapore 119260 (e-mail: elemaj@nus.edu.sg).

H. N. Phyu is with the Electrical Machines and Drives Laboratory, Department of Electrical and Computer Engineering, National University of Singapore, Singapore 119260 (e-mail: engp0570@nus.edu.sg).

Z. J. Liu and C. Bi are with the Data Storage Institute, National University of Singapore, Singapore 117608 (e-mail: dsiliuzj@dsi.nus.edu.sg; dsiliuzj@dsi.nus.edu.sg).

Digital Object Identifier 10.1109/TIA.2004.827478

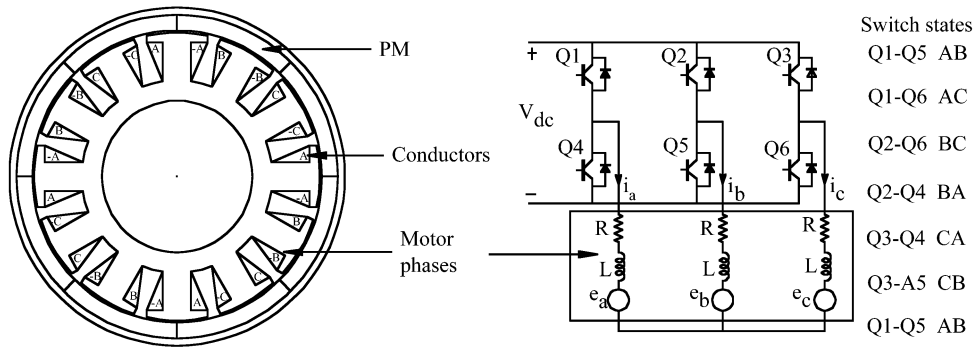


Fig. 1. BLDC motor configuration and the inverter circuit.

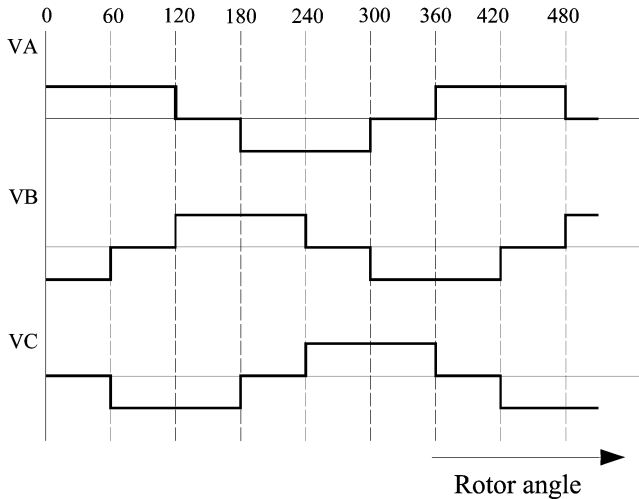


Fig. 2. Typical input voltage waveforms.

conducting at any instant. Hence, in order to predict both steady-state and dynamic performance for the BLDC motors, external circuit and rotor rotation should be coupled with the electromagnetic field. Fig. 1 shows the configuration of the BLDC motor and the inverter circuit with predefined switching states. The typical input voltage waveforms are shown in Fig. 2.

B. Current-Fed 2-D Complex Eddy-Current Model

As mentioned before, while only the steady-state solution may be of interest, it may take many cycles of computation before starting transients disappear. This excessive computation time required to reach the steady-state solution has prompted an interest in the traditional current-fed 2-D FEM complex eddy-current model (frequency-domain model). One motivation is that the steady-state solution in the frequency domain can be used as a starting point for the time-stepping solver.

2-D eddy-current phenomena are described by the diffusion equation. For the steady-state time harmonic case, this equation, in terms of the magnetic vector potential is given by

$$\frac{1}{\mu} \frac{\partial^2 A}{\partial x^2} + \frac{1}{\mu} \frac{\partial^2 A}{\partial y^2} = -J + j\omega\sigma A \quad (1)$$

where A is the axial component of the magnetic vector potential and μ is the permeability of the material. The first term on the right-hand side is the applied source current density and the last term is induced eddy-current density. By solving the diffusion

equation (1) using traditional FEM procedure, one can get the magnetic vector potential A for all the nodes in the solution region. After obtaining a solution from the frequency domain, an instant of time was chosen and the time-stepping solver was started with these vector potential results for initial conditions [18].

C. Time-Stepping FEM Model

1) *Modeling of the Electromagnetic Field:* The governing equation of the magnetic field is represented by Maxwell's equation in the form of a magnetic vector potential as

$$\nabla \times (\nu \nabla \times A) = J \quad (2)$$

where A is the axial component of the magnetic vector potential, J is the current density, and ν is the reluctivity of the material.

In the area of the stator conductor, the magnetic field equation can be represented as

$$\nabla \times (\nu \nabla \times A) + \frac{i_s}{S} = 0. \quad (3)$$

In iron cores and air-gap area, the magnetic field can be expressed as

$$\nabla \times (\nu \nabla \times A) + \sigma \frac{\partial A}{\partial t} = 0. \quad (4)$$

In the air gap and laminated stator iron core, the term $\sigma(\partial A/\partial t)$ is zero. It can only exist in the solid rotor iron core where eddy currents cannot be ignored.

There are two models which are commonly used to represent permanent magnets: a magnetization vector and an equivalent current sheet. Magnetizing vector method is used in this model. By using the magnetization vector method [18], the permanent magnet can be represented as an equivalent magnet current source as

$$\nabla \times (\nu \nabla \times A) = \nabla \times (\nu B_r). \quad (5)$$

In (2)–(4), i_s is the stator phase current, S is the total cross-sectional area of one turn on one coil side, σ is the conductivity of the material, and B_r is the remanent flux density of the permanent magnet.

2) *Circuit Equation:* The stator phase circuit equation for the proposed BLDC motor is

$$V_s = Ri_s + L\sigma \frac{di_s}{dt} + e \quad (6)$$

where R is the total stator resistance of one phase winding, L_σ is the inductance of the end windings, i_s is the stator current, and V_s is the supply voltage and e is the back electromotive force (EMF).

Back EMF can be represented as

$$e = \frac{l}{S} \left(\iint_{\Omega^+} \frac{\partial A}{\partial t} d\Omega - \iint_{\Omega^-} \frac{\partial A}{\partial t} d\Omega \right) \quad (7)$$

where l is the axial length of the iron core; Ω^+ and Ω^- are, respectively, the total cross-sectional areas of the go and return side of the stator phase conductors of the coils.

3) *Motion Equation*: The motion equation is

$$J_m \frac{d\omega}{dt} = T_e - T_L \quad (8)$$

where J_m is the moment of inertia, ω is the rotor speed, T_e is the electromagnetic torque, and T_L is the load torque.

The solution of the field equations (3)–(5) are obtained by minimizing the corresponding nonlinear energy functional. The minimization is performed by means of FEM using first-order triangular elements. Finite-element formulations are discussed in the next section.

D. Finite-Element Formulation

The variational approach and the Galerkin's approach are the two most popular methods to derive the element matrix equations. In this proposed model, the Galerkin's method is employed for the finite-element formulation. This is the particular weighted residual method for which the weighting functions are the same as the shape functions. According to the Galerkin's method, the magnetic vector potential can be expressed as

$$A = \sum_{i=1}^3 N_i A_i \quad (9)$$

where N_i are the element shape functions and the A_i are the approximations to the vector potentials at the nodes of the elements.

The *Galerkin's formulation* of the stator conductor field equation is

$$\iint \left[\frac{\partial N_i}{\partial x} \frac{\partial}{\partial x} \nu \sum_{j=1}^3 N_j A_j + \frac{\partial N_i}{\partial y} \frac{\partial}{\partial y} \nu \sum_{j=1}^3 N_j A_j + N_i \left(\frac{i_s}{S} \right) \right] dx dy = 0. \quad (10)$$

Alternatively, in matrix form,

$$\left[\nu[G]\{A\} + \{Q\} \frac{i_s}{S} \right] = 0. \quad (11)$$

For laminated stator iron core and air gap,

$$\iint \left[\frac{\partial N_i}{\partial x} \frac{\partial}{\partial x} \nu \sum_{j=1}^3 N_j A_j + \frac{\partial N_i}{\partial y} \frac{\partial}{\partial y} \nu \sum_{j=1}^3 N_j A_j \right] dx dy = 0. \quad (12)$$

In matrix form,

$$[\nu[G]\{A\}] = 0. \quad (13)$$

For the rotor iron core,

$$\iint \left[\frac{\partial N_i}{\partial x} \frac{\partial}{\partial x} \nu \sum_{j=1}^3 N_j A_j + \frac{\partial N_i}{\partial y} \frac{\partial}{\partial y} \nu \sum_{j=1}^3 N_j A_j \right] + \iint \left[\sigma N_i \left(\frac{\partial A_i}{\partial t} \right) \right] dx dy = 0. \quad (14)$$

In matrix form,

$$\left[\nu[G]\{A\} + \sigma[T] \left\{ \frac{\partial A}{\partial t} \right\} \right] = 0. \quad (15)$$

For the permanent magnet,

$$\iint_{\Omega} \nu \left(\frac{\partial A}{\partial x} \frac{\partial N_i}{\partial x} + \frac{\partial A}{\partial y} \frac{\partial N_i}{\partial y} \right) dx dy = \iint_{\Omega} \left(\nu \mu_o \left(M_x \frac{\partial N_i}{\partial y} - M_y \frac{\partial N_i}{\partial x} \right) \right) dx dy. \quad (16)$$

In matrix form,

$$\nu[G]\{A\} = \frac{\nu}{2} (B_{rx}[c_i] - B_{ry}[b_i]). \quad (17)$$

For the circuit equation,

$$V_s = \frac{l}{s} \left[\iint_{\Omega^+} N_i \frac{\partial A}{\partial t} d\Omega - \iint_{\Omega^-} N_i \frac{\partial A}{\partial t} d\Omega \right] + Ri + L_\sigma \frac{di_s}{dt}. \quad (18)$$

In matrix form,

$$V_s = \frac{l}{s} \left[\left(\{Q\} \left\{ \frac{\partial A}{\partial t} \right\} \right)_{\Omega^+} - \left(\{Q\} \left\{ \frac{\partial A}{\partial t} \right\} \right)_{\Omega^-} \right] + Ri_s + L_\sigma \frac{di_s}{dt} \quad (19)$$

where

$$T_{ij} = \iint N_i N_j dx dy = \begin{cases} \frac{\Delta_e}{6} & i = j \\ \frac{\Delta_e}{12} & i \neq j \end{cases}$$

$$Q = \iint N_i dx dy = \frac{\Delta_e}{3}$$

$$G = \iint \left(\frac{\partial N_i}{\partial x} \frac{\partial N_j}{\partial x} + \frac{\partial N_i}{\partial y} \frac{\partial N_j}{\partial y} \right) dx dy = \frac{b_i b_j + c_i c_j}{4\Delta_e}$$

and Δ_e is the triangular area of the element.

E. Time Discretization

The field equations (11), (13), (15), and (17), the circuit equation (19), and the motion equation (8) are time dependent. These equations are needed to discretize in the time domain. The method of discretization used is based on the following equations [18]:

$$\beta \left\{ \frac{\partial A}{\partial t} \right\}^{t+\Delta t} + (1 - \beta) \left\{ \frac{\partial A}{\partial t} \right\}^t = \frac{\{A\}^{t+\Delta t} - \{A\}^t}{\Delta t}. \quad (20)$$

Basically, there are three different types of time discretization:

- 1) forward difference type ($\beta = 0$);
- 2) backward difference type ($\beta = 1$);
- 3) Crank–Nicholson method ($\beta = 1/2$).

The backward difference type is used in this model because it has a good convergence rate.

F. Linearization

In the analysis of the electrical machines, the problems are almost always nonlinear due to the presence of ferromagnetic materials. Good designs will typically operate at or near the saturation point. The magnetic permeability or reluctance is non-homogenous and will be a function of the local magnetic fields which are unknown at the start of the problem. The most popular method of dealing with nonlinear problems in magnetic is the Newton–Raphson method [18]. In this model, field equations are nonlinear; linearization of these equations is required before they can be combined with other equations of the system in a global matrix equation. Newton–Raphson procedure is applied to linearize the nonlinear system equations. A cubic spline interpolation algorithm is used to represent the magnetization curve of the ferromagnetic materials.

Newton-Raphson form of the stator conductor field equation after time discretization is

$$\nu[G][\Delta A]_{k+1}^{t+\Delta t} + \frac{[Q]}{S}[\Delta I]_{k+1}^{t+\Delta t} = -\nu[G][A]_k^{t+\Delta t} - \frac{[Q]}{S}[\Delta I]_k^{t+\Delta t}. \quad (21)$$

In the laminated stator iron core and air gap,

$$\nu[G][\Delta A]_{k+1}^{t+\Delta t} = -\nu[G][A]_k^{t+\Delta t}. \quad (22)$$

In the solid rotor iron core,

$$\nu[G][\Delta A]_{k+1}^{t+\Delta t} + \frac{\sigma[T]}{\Delta t}[\Delta A]_{k+1}^{t+\Delta t} = -\nu[G][A]_k^{t+\Delta t} - \frac{\sigma[T]}{\Delta t}[\Delta A]_k^{t+\Delta t}. \quad (23)$$

In the permanent magnets, the equation is

$$\nu[G][\Delta A]_{k+1}^{t+\Delta t} = -\nu[G][\Delta A]_k^{t+\Delta t} + \frac{\nu}{2}(B_{rx}[c_i] - B_{ry}[b_i]) \quad (24)$$

and the stator circuit equation is given by

$$\begin{aligned} & [\Delta I]_{k+1}^{t+\Delta t} R + \frac{L}{\Delta t}[\Delta I]_{k+1}^{t+\Delta t} + \frac{[Q]}{S}l \frac{[\Delta A]_{k+1}^{t+\Delta t}}{\Delta t} \\ & = -[I]_k^{t+\Delta t} R - \frac{L}{\Delta t}[I]_k^{t+\Delta t} - \frac{[Q]}{S}l \frac{[A]_k^{t+\Delta t}}{\Delta t} \\ & + V + \frac{L}{\Delta t}[I]^t + \frac{[Q]}{S}l \frac{[A]^t}{\Delta t}. \end{aligned} \quad (25)$$

G. Mesh Generation and Rotation

Mesh generation for the FEM should be simple, robust, and rotor mesh should be allowed to rotate easily. In this approach, the FEM mesh of the cross section of the BLDC motor is divided

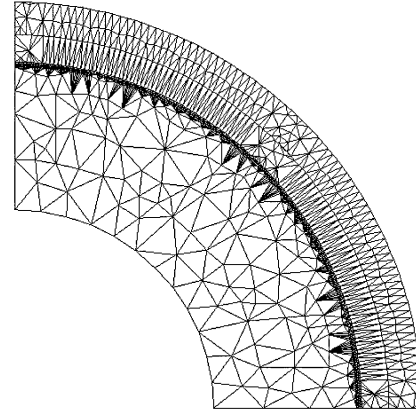


Fig. 3. FEM mesh before rotor rotation (1899 nodes, 2828 elements).

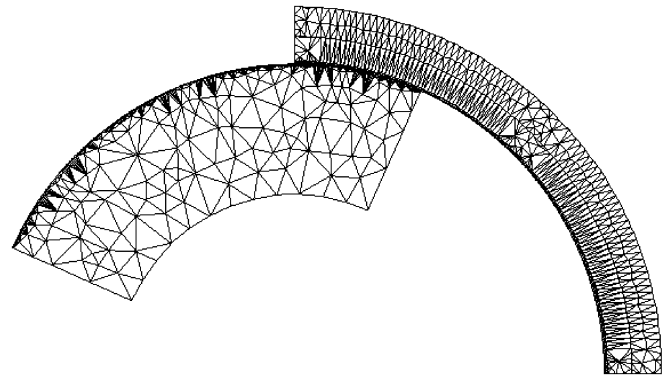


Fig. 4. FEM mesh after rotation 5000 steps.

into two parts: the stator and the rotor, with each including a part of the air gap. Meshes of the two parts are then generated separately. The air gap is divided into three layers: two upper layers belong to the rotor and the rest layer belongs to the stator. The inner most nodes of the rotor mesh and the outer most nodes for the stator mesh are connected by the periodic boundary condition (Fig. 3). When the rotor is rotated according to the time step, the shape of the mesh for both the stator and rotor can be kept constant and only the coordinates of the rotor mesh and the periodic boundary condition on the interface are needed to change. The motor mesh after rotation with 5000 steps is shown in (Fig. 4). Therefore, in this approach the stator mesh and the rotor mesh are required to generate only one time and it can greatly reduce the computing time required to generate the FEM mesh at each time step [14], [15].

H. Coupling the Rotor Movement With the FEM

After time discretization, the motion equation (8) can be represented by

$$\omega^k = \omega^{k-1} + \left(\frac{T_e - T_L}{J} \right) \times \Delta T \quad (26)$$

and rotor displacement can be determined by the following equations:

$$\Delta \theta_m = \omega^k \times \Delta T \quad (27)$$

$$\theta_m^k = \theta_m^{k-1} + \Delta \theta_m \quad (28)$$

TABLE I
MOTOR SPECIFICATIONS

Voltage	12V
No. of poles	8
No. of slots	12
Rated speed	7200 rpm
Stator outside diameter	28 mm
Rotor outside diameter	30 mm
Stack length	4.5 mm
Air gap length	0.2mm

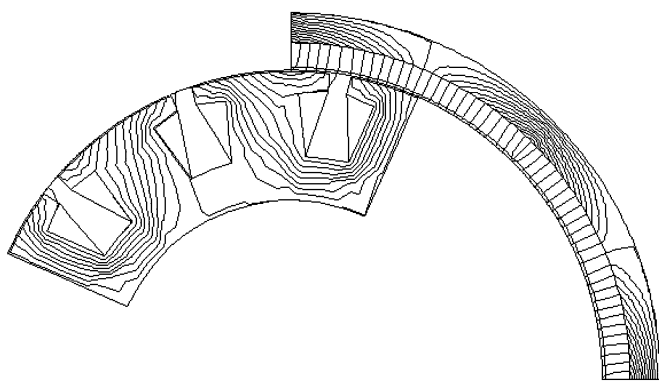


Fig. 5. Computed steady-state flux distribution.

where θ_m is the rotor angle. This step has been carried out in the post-processing process. The procedure is as follows.

- 1) Calculate the electromagnetic torque (T_e) first by using Maxwell stress tensor method.
- 2) Use the motion equation after time discretization (26) to calculate the rotor speed.
- 3) From that, calculate the rotor displacement (rotor angle) according to (27) and (28).

The rotor FEM mesh is moved according to the rotor angle θ_m at every time steps.

III. SOLUTION OF THE SYSTEM OF EQUATIONS

Field equations (21)–(24), and the circuit equation (25) have to be solved simultaneously. Rotor movement has to be coupled by using (26)–(28). The coefficient matrix is symmetric, banded and nonzeros terms are clustered around the main diagonal. Hence, for the iterative solver, only the upper triangular coefficient matrix with nonzero elements is stored. At each iteration cycle, the Incomplete Cholesky Conjugate Gradient (ICCG) algorithm is used to solve the large system of equations. In steady-state performance calculation, the magnetic vector potentials gotten from the frequency-domain analysis are used as the initial values for the time-stepping iterative solver. In dynamic performance calculation, especially for detailed analysis of the starting period, the initial conditions are started from zero.

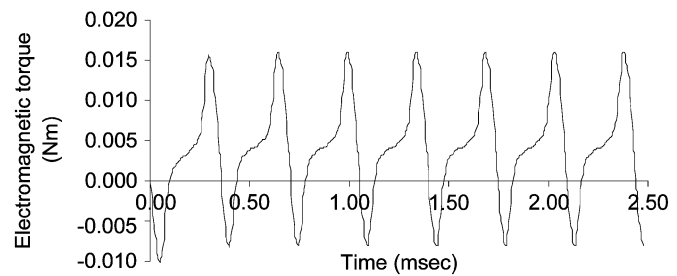


Fig. 6. Computed electromagnetic torque at no-load condition.

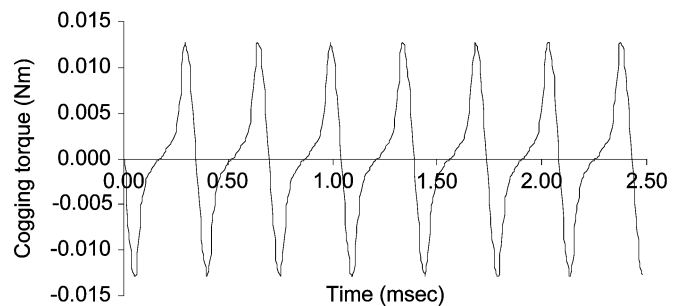


Fig. 7. Computed cogging torque.

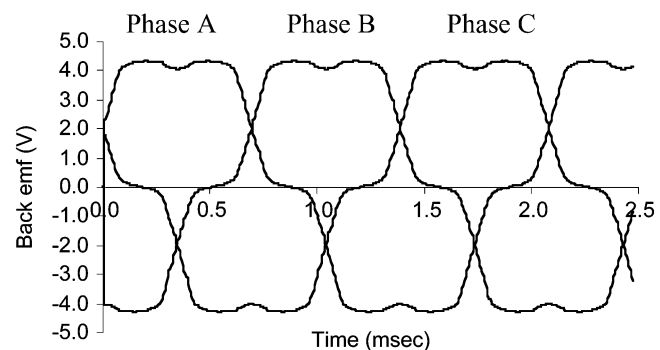


Fig. 8. Computed back EMF.

IV. ANALYSIS AND DISCUSSION OF RESULTS

The developed model has been used to simulate the steady-state and transient conditions of the exterior rotor BLDC motor. Motor specifications are listed in Table I. Because of the motor symmetry only one quadrant is used as a solution domain. The computed steady-state flux distribution is shown in Fig. 5. Forces and torques are calculated by integrating the Maxwell's stress tensors along a closed path in the air gap [19], [20]. The cogging torque is calculated when there is no armature current in the stator winding. The simulated steady-state electromagnetic torque, the cogging torque, and the back EMF are shown in Figs. 6–8, respectively. The calculated and measured stator phase currents at no-load condition are shown in Fig. 9. It can be seen that the computed and measured results agree closely. The motor transient responses at starting, during load changes, and input voltage variations are also computed and presented in Figs. 10–13.

A. Motor Starting Condition

The developed dynamic model has been used to investigate the starting condition of the motor. In order to start up the motor

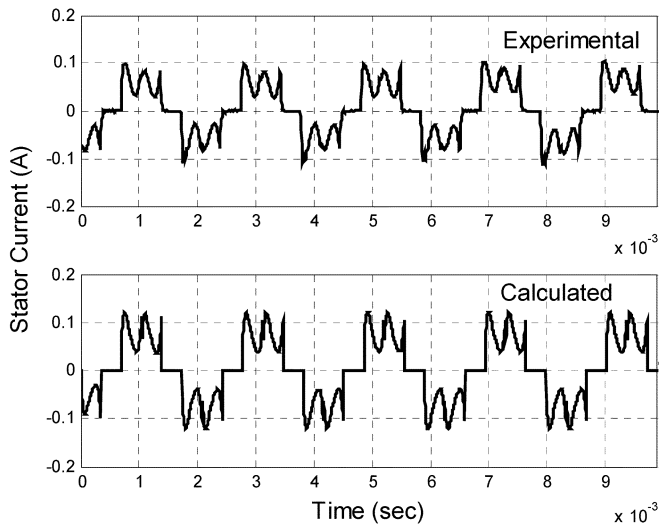
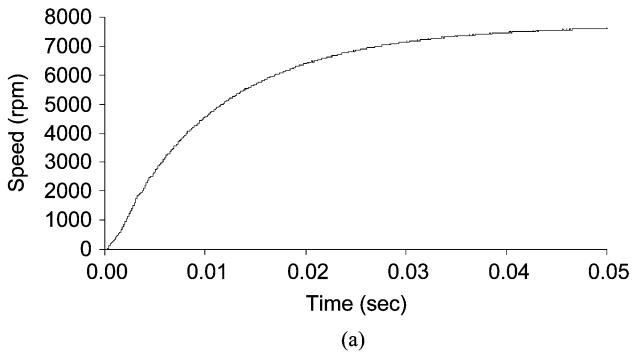
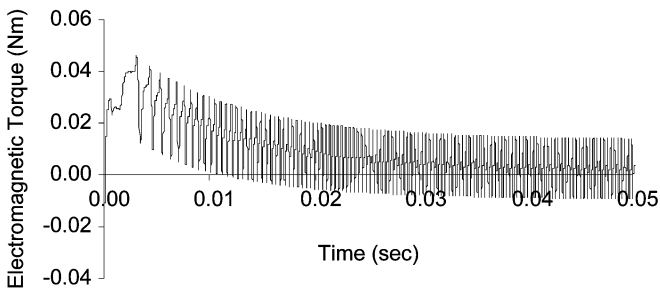


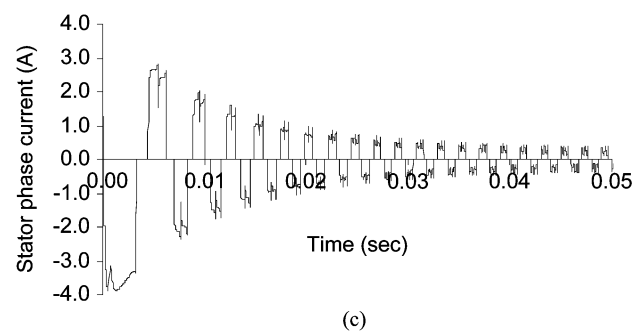
Fig. 9. Experimental and calculated stator phase current.



(a)



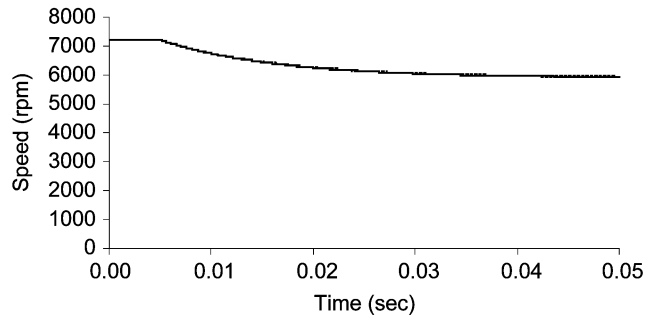
(b)



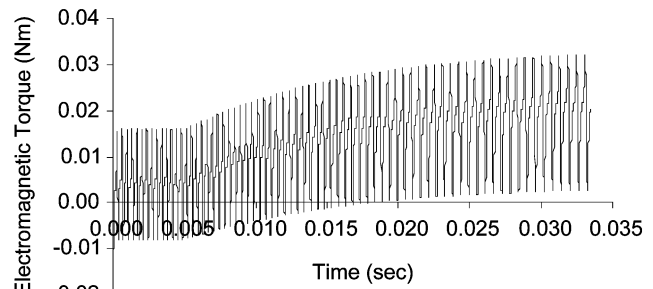
(c)

Fig. 10. Motor transient at starting condition. (a) Speed. (b) Torque. (c) Stator phase current.

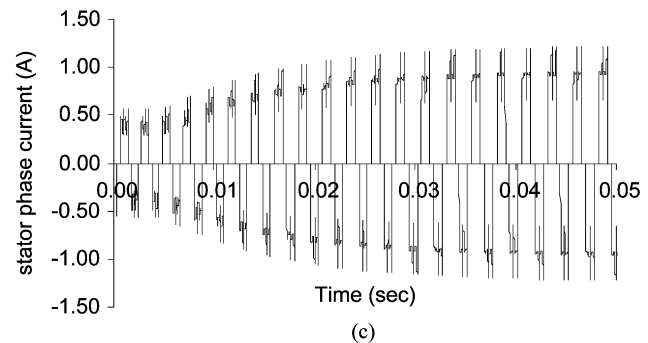
from the rest position to full speed quickly, the starting torque must be significantly more than the running torque. The simulation results for the starting condition of the angular speed of the



(a)



(b)



(c)

Fig. 11. Motor transient response due to an increase in the load torque. (a) Speed. (b) Torque. (c) Stator phase current.

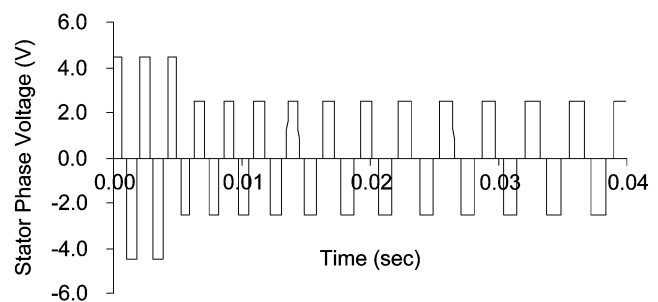


Fig. 12. Step voltage change.

rotor, the stator phase currents, and the electromagnetic torque are also shown in Fig. 10.

B. Simulation of Changing the Mechanical Load Torque

The response was verified for a step increase of the mechanical load torque from 0.002 to 0.01 N·m when the stator phase

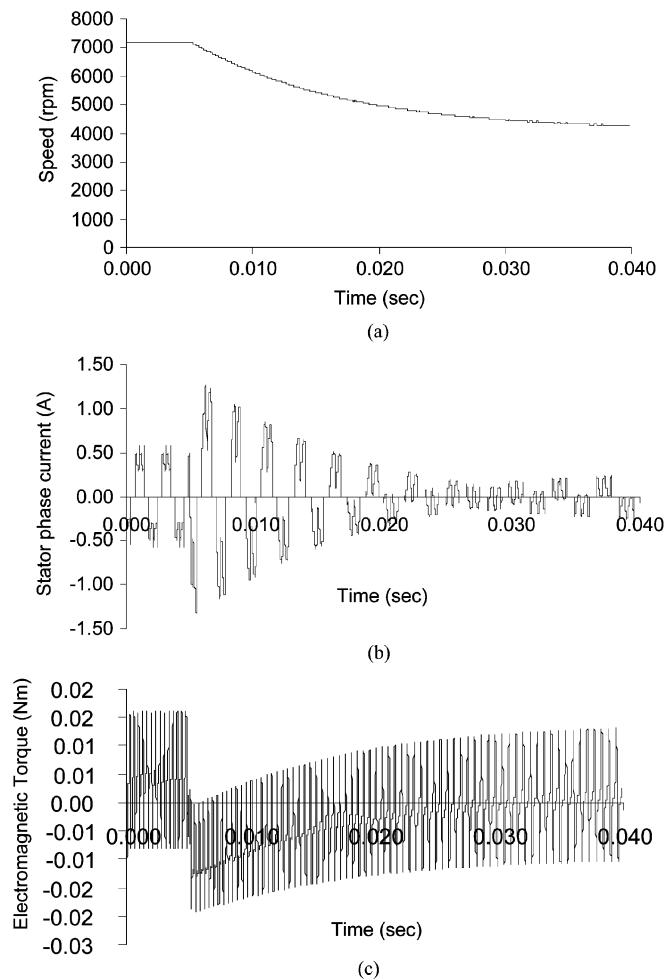


Fig. 13. Motor transient response during a sudden reduction of supply voltage. (a) Speed. (b) Stator phase current. (c) Electromagnetic torque.

voltage is 4.5 V and the rated speed is 7200 r/min. The simulation results are shown in Fig. 11.

C. Step Voltage Variation

This situation could arise when the motor speed is controlled through voltage. Figs. 12 and 13 show the current, torque, and speed transients when the motor is loaded and the input voltage is dropped from 4.5 to 2.5 V. It can be seen that both current and torque instantaneously reverse their direction because the new voltage is lower than the generated EMF in the winding at the instant of voltage changed. The speed also goes down.

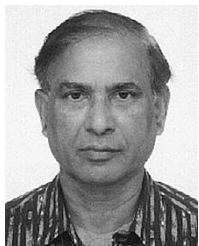
V. CONCLUSION

A dynamic model for the BLDC motor has been developed using the time-stepping FEM. In the proposed model, the external circuit equations and the motion equation are coupled together with the electromagnetic field equations and solved simultaneously. Using the developed model, the dynamic performances of the motor have been studied at starting, for load torque changes, and for variation in input voltage. Simulation

and experimental results presented in the paper show close agreement.

REFERENCES

- [1] N. A. Demerdash and T. W. Nehl, "Dynamic modeling of brushless DC motors for aerospace actuation," *IEEE Trans. Aerosp. Electron. Syst.*, vol. AES-16, pp. 811–821, Nov. 1980.
- [2] M. A. Jabbar, T. S. Low, and M. Rahman, "Permanent magnet motors for brushless operation," in *Conf. Rec. IEEE-IAS Annu. Meeting*, 1988, pp. 15–19.
- [3] P. Pillay and R. Krishnan, "Application characteristics of permanent magnet synchronous and brushless DC motors for servo drives," *IEEE Trans. Ind. Applicat.*, vol. 27, pp. 986–996, Sept./Oct. 1991.
- [4] M. A. Rahman and P. Zhou, "Analysis of brushless permanent magnet synchronous motors," *IEEE Trans. Ind. Electron.*, vol. 43, pp. 256–266, Apr. 1996.
- [5] S. C. Park, B. I. Kwon, H. S. Yoon, S. H. Won, and Y. G. Kang, "Analysis of exterior rotor BLDC motor considering the eddy current effect in the rotor steel shell," *IEEE Trans. Magn.*, vol. 35, pp. 1302–1305, May 1999.
- [6] Z. Q. Zhu, D. Howe, and C. C. Chan, "Improved analytical model for predicting the magnetic field distribution in brushless permanent magnet machines," *IEEE Trans. Magn.*, vol. 38, pp. 229–238, Jan. 2002.
- [7] T. J. E. Miller, M. Popescu, C. Cossar, M. McGilp, and J. A. Walker, "Calculating the interior permanent-magnet motor," in *Proc. Electrical Machines and Drives Conf. (IEMDC'03)*, vol. 2, Madison, WI, June 2003, pp. 1181–1187.
- [8] S. P. Lim and K. J. Tseng, "Dynamic model of interior permanent magnet motor with skewed stator slots," in *Proc. IEEE IECON'99*, vol. 3, 1999, pp. 1471–1476.
- [9] S. J. Salon and J. D. Angelo, "Applications of the hybrid finite element-boundary element method in electromagnetic," *IEEE Trans. Magn.*, vol. 24, pp. 80–85, Jan. 1988.
- [10] A. Boglietti, M. Chiampi, D. Chiarabaglio, and M. Tartaglia, "Finite element analysis of permanent magnet motors," *IEEE Trans. Magn.*, vol. 25, pp. 3584–3586, Sept. 1989.
- [11] P. Zhou, M. A. Rahman, and M. A. Jabbar, "Field circuit analysis of permanent magnet synchronous motors," *IEEE Trans. Magn.*, vol. 30, pp. 1350–1359, July 1994.
- [12] J. Gan, K. T. Chau, Y. Wang, C. C. Chan, and J. Z. Jian, "Design and analysis of a new permanent magnet brushless DC machine," *IEEE Trans. Magn.*, vol. 36, pp. 3353–3356, Sept. 2000.
- [13] M. Dai, A. Keyhani, and T. Sebastian, "Torque ripple analysis of a permanent magnet brushless DC motor using finite element method," in *Proc. Electric Machines and Drives Conf. (IEMDC 2001)*, 2001, pp. 241–245.
- [14] S. L. Ho and W. N. Fu, "Review and future application of finite element method in the induction motor," *Elect. Mach. Power Syst.*, vol. 26, no. 2, pp. 111–125, 1998.
- [15] S. L. Ho, W. N. Fu, and H. C. Wong, "Direct modeling of the starting process of skewed rotor induction motors using a multi slice technique," *IEEE Trans. Magn.*, vol. 14, pp. 1253–1258, Dec. 1999.
- [16] Y. Wang, K. T. Chau, C. C. Chan, and J. Z. Jiang, "Transient analysis of a new outer-rotor permanent-magnet brushless DC drive using circuit-field-torque coupled time-stepping finite-element method," *IEEE Trans. Magn.*, vol. 38, pp. 1297–1300, Mar. 2002.
- [17] L. Xu and W. N. Fu, "Evaluation of third harmonic component effects in five phase synchronous reluctance motor drive using time stepping finite element method," *IEEE Trans. Ind. Applicat.*, vol. 38, May/June 2002.
- [18] S. J. Salon, *Finite Element Analysis of Electrical Machines*. Norwell, MA: Kluwer, 1995.
- [19] M. Marinescu and N. Marinescu, "Numerical computation of torques in permanent magnet motors by Maxwell stresses and energy method," *IEEE Trans. Magn.*, vol. 24, pp. 463–466, Jan. 1988.
- [20] M. Antila, E. Lantto, and A. Arkkio, "Determination of forces and linearized parameters of radial active magnetic bearings by finite element technique," *IEEE Trans. Magn.*, vol. 34, pp. 684–694, May 1998.
- [21] P.-B. Zhou, *Numerical Analysis of Electromagnetic Fields*. Berlin, Germany: Springer-Verlag, 1993.



M. A. Jabbar (SM'84) was born in Sylhet, Bangladesh. He received the B.Sc.Eng. degree from Bangladesh University of Engineering and Technology (BUET), Dhaka, Bangladesh, and the Ph.D. degree from the University of Southampton, Southampton, U.K.

He was a Lecturer at BUET for a number of years. He is currently an Associate Professor of electrical engineering at the National University of Singapore, Singapore. He has worked in research and practice for more than 30 years in Bangladesh, the U.K., and

Singapore. He has extensive experience in motor design and development. His area of research interest is small motor design and manufacture. He has worked in the appliance industry in the U.K. as a Senior Designer of small motors. He worked in spindle motor design and manufacture for Maxtor Corporation for five years as the Manager and then as the Director of R&D. His special interests are magnetics and computation. He has authored numerous research papers published in international conference proceedings and journals. He is the holder of a number of patents on special types of motors. Currently, he is engaged in research and teaching concerning electric machines and engineering magnetics.

Dr. Jabbar is a Corporate Member of the Institution of Electrical Engineers, U.K., and a Chartered Engineer in the U.K. He is also a Fellow of The Institute of Engineers, Bangladesh. He was the recipient of a Commonwealth Scholarship during 1972–1975.



Hla Nu Phyu (S'02) received the B.Eng. degree in electrical power engineering from Yangon Technological University, Yangon, Myanmar, in 1998. She is currently working toward the Ph.D. degree in electrical engineering in the Department of Electrical and Computer Engineering, National University of Singapore, Singapore.

Her research interests include computational analysis, electromagnetic field modeling, finite-element analysis and numerical modeling, and analysis of small PM motors.



Zhe Jie Liu (M'94–SM'99) received the Ph.D. degree from Liverpool University, Liverpool, U.K., in 1992.

He was a Research Associate at Sheffield University, working in the area of computer-aided design of permanent-magnet motors and drives. He is presently a Research Scientist with the Data Storage Institute, National University of Singapore, Singapore. His research interests include computational electromagnetics, design optimization, magnetic recording processes, and distributed/collaborative

computing.



Chao Bi (M'96) received the B.Eng. degree from Hefei Industrial University, Hefei, China, in 1982, the M.Eng. degree from Xi'an Jiaotong University, Xi'an, China, in 1984, and the Ph.D. degree from the National University of Singapore, Singapore, in 1994.

He is presently a Research Scientist in the Data Storage Institute, National University of Singapore, Singapore. His research interests include electromagnetic field synthesis and analysis, micro permanent-magnet motor design and control, micro actuator design and control, and optimization technology.